

Simulations for proton detection in $^{59}\text{Fe}(d,p)^{60}\text{Fe}$

A.B. McIntosh

This report describes simulations done in preparation for an experiment to measure the gamma ray strength function of ^{60}Fe . Iron-60 is of interest in s-process nucleosynthesis since this is a branch point, and therefore impacts the abundances of heavier elements. Iron-60 has been observed in the gamma spectrum nearby in our galaxy [1]. Iron-60 has been measured in sea floor sediments across the globe, and on the surface of the moon [2,3]. Iron-60 has also been observed in cosmic rays [4]. These findings all imply that ^{60}Fe was produced in the relatively recent past and distributed in our region of the galaxy, and by studying it we may learn about s-process nucleosynthesis.

Measurement of the gamma ray strength function in reactions of $^{57}\text{Fe}(d,p)^{58}\text{Fe}$ and $^{59}\text{Fe}(d,p)^{60}\text{Fe}$ will be made at TAMU. To measure the excitation energy, we will measure the energy and angle of the recoil proton at backward angles in the lab frame using an annular silicon detector (S3 from Micron Semiconductor). Consideration of background reactions is assessed in another 2019 TAMU annual report [5].

The excitation energy resolution is determined by several factors: the energy resolution of the silicon detector, the angular resolution of the silicon detector, the finite width of the beam-spot on target, the depth of the reaction point in the target, the energy loss of the proton in the target, and the energy loss of the proton in the dead layer of the silicon detector. To assess the impact of these factors, a simple simulation was developed. The radioactive beam is considered to impinge on the target with a Gaussian distribution with a width of 5mm (FWHM). The reaction point in the target is chosen uniformly within the thickness of the target (1000ug/cm²). The excitation energy of the ^{60}Fe is chosen at specific discrete values selected by the user (7.0MeV and 9.5MeV). The energy of the recoil proton is determined by conservation of energy (including Q value, which is a significant contribution). The angle of the proton is selected in the CM frame on a distribution described by TWOFNR calculations (a DWBA (Distorted Wave Born Approximation) code) for angular momenta of 1, 2, 3 and 4 hbar. A cos(theta) weighting is applied, which dominates the angular yield distribution. The proton loses an appropriate amount of energy as it exits the previously chosen fraction of the target at the appropriate angle in the lab frame. The proton loses energy in the dead layer of the silicon detector (8000 Angstroms, with random fluctuations of 800 Angstroms). The proton then loses its remaining energy in the silicon detector in a specific ring segment. The S3 silicon detector contains 24 ring segments between 22mm and 70mm radius, and is positioned 2 cm upstream of the target. The sector side must face the target since the ring side has a much thicker dead-layer. The energy is smeared by sampling a Gaussian with width 50 keV. The center of the ring is used as the measured angle relative to the ideal target location (this is the best the experimenter would be able to do). This "measured" angle and smeared energy is used to back correct for energy loss in the dead silicon (this time neglecting the unknown fluctuations) and for energy loss in the target (assuming the reaction occurred at the center of the target in all three dimensions). This corrected energy and angle are used to calculate the excitation energy of the ^{60}Fe .

Fig. 1 (left) shows the correlation between the true energy and angle of the proton in the lab frame for $E^* = 7.0$ MeV and $E^* = 9.5$ MeV. The lowest energy (around 500 keV) protons are at 180 degrees. The neutron separation energy for ^{60}Fe is at $E^* = 8.8$ MeV. States above this are not strictly necessary for the analysis but are helpful as a check of the measurement, as the gamma decay branch decreases as the neutron decay branch turns on. The right panel of Fig. 1 shows the same energy-angle correlation after considering the finite acceptance of the detector and all the factors noted above. The distribution is cut out except within 120-150 degrees. The proton energy is diminished and broadened. Some very low energy protons that would otherwise strike the detector are stopped before they reach the active part of the silicon.

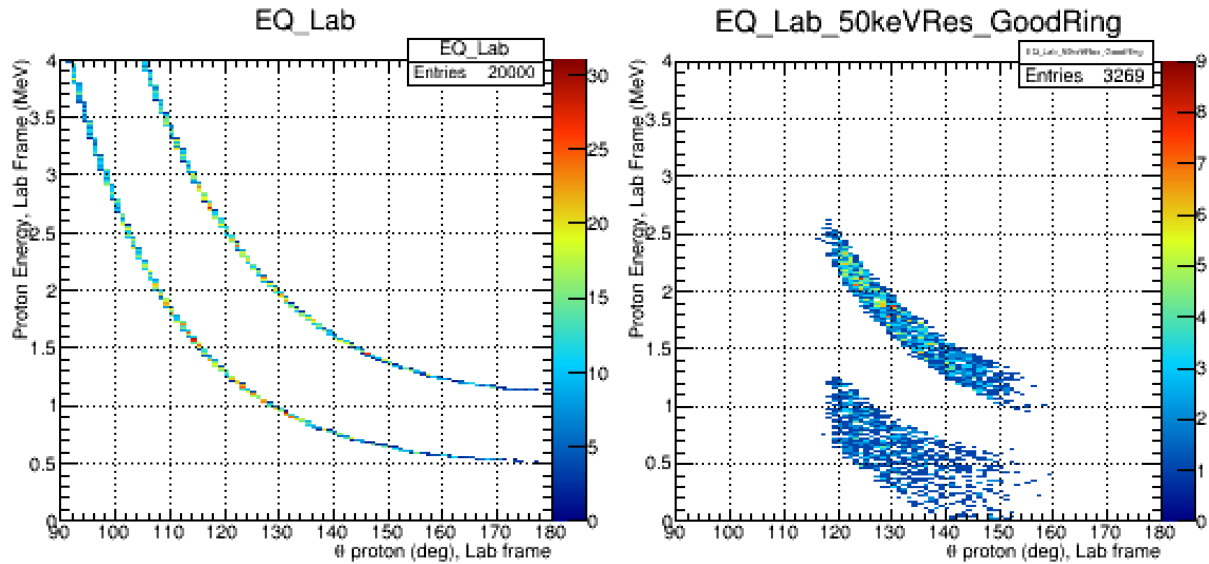


FIG. 1. Energy-angle correlation of the proton from $^{59}\text{Fe}(d,p)^{60}\text{Fe}$ @ 7.5 MeV/u for "perfect" detectors (left) and "reasonable" detectors (right).

Using the values "measured" in Figure 2 (left) to calculate the excitation energy resolution gives around 270 keV (σ) at $E^* = 7.0$ MeV and between 350 and 450 keV at $E^* = 9.5$ MeV (the width depends on the ring, with worse resolution for larger angles). Since we are not looking for discrete states, but only need to select on a region of excitation energy in the analysis (the Forward Analysis Method), this resolution expected is acceptable.

We now consider the rate of good measured events, summarized in Table I. Assuming a beam intensity of $1E5$ pps, a cross section of 27.8 mb (obtained from the TWOFNR calculations mentioned above), and a target thickness of 1000 $\mu\text{g}/\text{cm}^2$, one expects a reaction rate of 0.2 reactions per second. The silicon efficiency is about 17% due entirely to the geometrical coverage. Assuming an efficiency for measuring gamma rays of 25%, we expect on the order of 5000 good measured reactions per week.

Table 1. Predicted reaction rate for $^{59}\text{Fe}(d,p)^{60}\text{Fe}$ @ 7.5 MeV/u.

N=lot		
Intensity	1.00E+05	particles/sec
Cross section	27.8	mb
	2.78E-26	cm²
Thickness	1000	ug/cm²
Thickness	0.001	g/cm²
molar mass	16	g/mol for CD₂
Thickness	0.0000625	molCD₂/cm²
NA	6.02E+23	moleculesCD₂/mol
Thickness	3.76E+19	moleculesCD₂/cm²
Thickness	7.53E+19	Dnuclei/cm²
Reaction Rate	2.09E-01	reactions/sec
silicon eff	17%	
BaF₂ efficiency	25%	
Residue Efficiency	100%	
Detected Reaction Rate	0.008891	reactions/sec
Detected Reaction Rate	32.01	reactions/hour
Detected Reaction Rate	224.05	reactions/day
Detected Reaction Rate	5377.15	reactions/week

[1] R. Diehl. Rep. Prog. Phys. **76**, 026301 (2013).

[2] A. Wallner *et al.*, Nature **532**, 69 (2016).

[3] L. Fimiani *et al.*, Phys. Rev. Lett. **116**, 151104 (2016).

[4] W.R. Binns *et al.*, Science **352**, 677 (2016).

[5] A.B. McIntosh, *Progress in Research*, Cyclotron Institute, Texas A&M University (2018-2019),p. II-